International Journal of Thermophysics, Vol. 15, No. 3, 1994

Thermal Diffusivity and Ultrasonic Velocity of Saturated R125

K. Kraft[1] **and A. Leipertz**[1]

Received October 22, 1993

We report—to the best of our knowledge—the first data for the thermal diffusivity and ultrasonic velocity of both phases of saturated R125 in the temperature range from 20 °C to the critical point. The data were obtained in thermodynamic equilibrium by applying dynamic light scattering.

KEY WORDS: light scattering; refrigerants; R125; thermal diffusivity; sound velocity.

1. INTRODUCTION

Since the utilization of the currently used full haloginated refrigerants was restricted in the Montreal Protocol of 1987, there is an urgent need for thermophysical properties of the most promising alternatives, which are the chlorine-free, haloginated carbon hydrogenes. R125 is a prospective substitute for R502 in commercial refrigeration and cold storage and for R22 in industrial refrigeration. Today no data for thermal conductivity or diffusivity and sound velocity are available for this refrigerant [1].

Dynamic light scattering allows the determination of both properties. As no macroscopic gradients are induced in the sample, measurements can be performed on the saturation line and in the critical region. We have measured both properties in the temperature range from 20°C to the critical temperature. As no other data sets are available, only data consistency can be used to check the accuracy of the method.

[1] Lehrstuhl für Technische Thermodynamik, Universität Erlangen-Nurenberg, Am Weichselgarten 9, D-91058 Erlangen, Germany.

0195-928X/94/0500-0387$07.00/0

2. METHOD

Dynamic light scattering is a well-established method for the determination of the thermal diffusivity of pure liquids and liquid mixtures [2–5]. In recent years the determination of the sound velocity has been established by using this method in the heterodyne mode [6–10].

The principle of the method is the detection of the power spectral density of the scattered light induced by a laser beam passing through the sample (Fig. 1). For a pure fluid, the width of the central unshifted Rayleigh line, which is caused by stochastic entropy fluctuations, is proportional to the thermal diffusivity. The frequency shift of the Brillouin lines, which are generated by microscopic pressure fluctuations (phonons), with respect to the Rayleigh line is proportional to the sound velocity and their widths to the sound attenuation constant [11]. All values depend on the modulus of the scattering vector **q**

$$q = \frac{4\pi n}{\lambda_0} \sin \frac{\theta_s}{2} \tag{1}$$

where θ_s in the scattering angle, λ_0 the wavelength of the laser in vacuum, and n the refractive index of the sample.

Because the width of the central Rayleigh line is too narrow to be measured in the frequency domain with reasonable accuracy, correlation techniques measuring in the time domain are to be preferred. Here the Fourier transform of the spectrum is observed, showing exponential decaying functions for each line. Each decay time is inversely proportional to the line width of the corresponding line in the frequency domain.

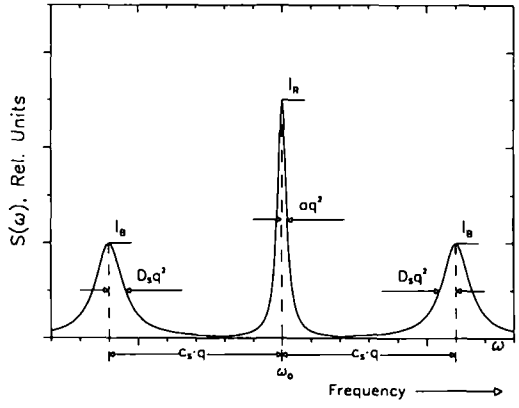

Fig. 1. Power spectral density of a pure fluid.

Figure 2 shows the experimental setup, which is similar to that described in some detail in Refs. 6–9. The sample fluid is put into a thermostated pressure vessel. The temperature is measured by means of a PT100 probe with a resolution of 0.01 K and an inaccuracy of ± 0.05 K. The temperature stability of the thermostat is better than 0.02 K over the time period of a single measurement. As all measurements are performed in the two-phase region, no pressure measurement is necessary. An argon ion laser working at $\lambda = 488.0$ nm in the sigle mode with a typical laser power of 250 mW is irradiated into the sample. In the critical region the power is reduced to 20 mW to avoid induced convention (see Section 4.1). The scattered light intensities are detected by two photomultiplier tubes (PMT). Two cross-correlation functions are computed by two correlators in parallel, offering the possibility of measuring at the same time in two different time scales, a helpful tool in investigating long-time distortions of the Rayleigh signal. Evaluating the cross-correlation function of the independent signals from two PMTs allows the suppression of dead time effects and of afterpulses of the PMTs in the measured correlogram. This is the only way to avoid influences in the Brillouin signal from the fast pressure fluctuations in the fluid.

The measured correlation function in general consists of several terms:

$$g(\tau) = (I_{R0} + I_R + 2I_B)^2 + I_R^2 \exp(-2\tau/\tau_{cR}) + 2I_{R0} I_R \exp(-\tau/\tau_{cR}) + 2I_B^2 \exp(-2\tau/\tau_{cB}) \tag{2}$$

Here τ_{cR} and τ_{cB} are the decay times of the Rayleigh and Brillouin signal, respectively, with intensities I_R and I_B, while I_{R0} is the intensity of the coherent background caused by reflections on the window surfaces of the pressure vessel, which are hard to avoid.

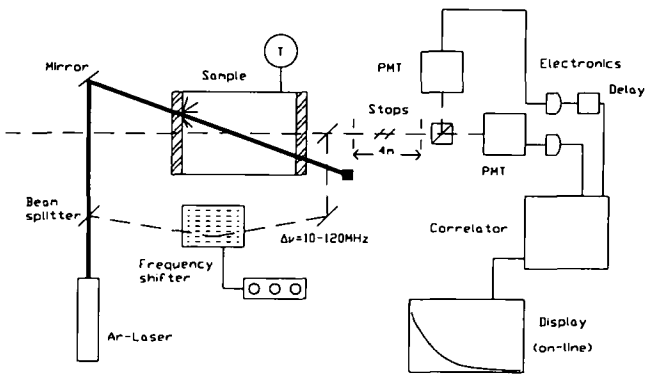

Fig. 2. Experimental setup.

An accurate analysis of the decay times containing information about the thermal diffusivity is almost impossible in this way. Also, the frequency shift of the Brillouin lines containing information on the sound velocity is not detectable. Adding a frequency-adapted background to the scattered light (heterodyne method) by employing a second beam path (Fig. 2) leads to the following forms of the convoluted correlation function, depending on the frequency of the reference beam.

2.1. Heterodyne Rayleigh Measurements

For determination of the thermal diffusivity the decay time of the central Rayleigh line must be measured. Adding a coherent unshifted background of sufficient intensity to the scattered light, the cross-correlation function can be written [12]

$$g(\tau) = (I_{R0} + I_R + 2I_B)^2 + 2I_{R0} I_R \exp(-\tau/\tau_{cR}) \tag{3}$$

which is a single exponential with a constant background:

$$g(\tau) = C + A \exp(-\tau/\tau_{cR}) \tag{4}$$

As an example, Fig. 3 shows an observed correlation function measured in this way.

Determination of the decay time τ_{cR} gives the thermal diffusivity according to

$$a = \frac{1}{\tau_{cR} q^2} \tag{5}$$

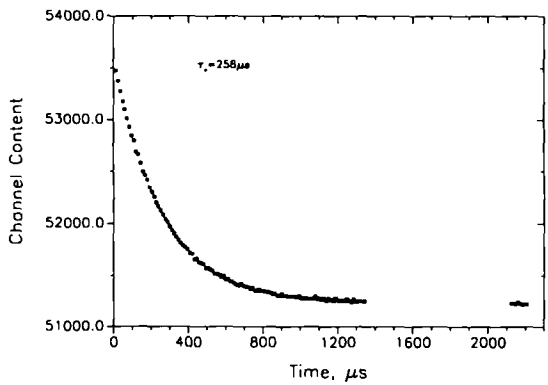

Fig. 3. Heterodyne Rayleigh measurement.

A newly developed multifit procedure [13] allows the exclusion of most systematic errors and leads to an accurate determination of τ_c.

For determination of the thermal diffusivity the modulus of the scattering vector **q** must be evaluated. For this, the index of refraction n must be known; see Eq. (1). Applying the law of refraction to the problem, however, the scattering angle Θ_s in Eq. (1) can be substituted by the incident angle at the entrance window Θ_e, leading to [8]

$$q = \frac{2\pi \sin \Theta_e}{\lambda_0 \cdot \cos[\frac{1}{2} \arcsin(\sin \Theta_e / n)]} \tag{6}$$

Here θ_e is the angle between the incident laser beam and the direction of observation measured by means of autocollimation with an error of less than 0.02°. Applying small angles ($\Theta_e < 7°$) the cos term containing the index of refraction can be neglected, introducing an error of less than 0.2%.

2.2. Heterodyne Brillouin Measurements

The sound velocity is related to the frequency difference between the Rayleigh and the Brillouin lines:

$$\Delta\varpi = c_s q \tag{7}$$

Here $\nu = \Delta\varpi/2\pi$ is the frequency of the sound waves detected. This value can be influenced by the angle of detection. Traditional methods observing the frequency shift of the Brillouin lines in a frequency-resolving way use angles of 90°, leading to frequencies in the GHz region. Here strong dispersion may occur. In dynamic light scattering, angles of 2 to 7° are applied, leading to measurement frequencies according to Fig. 4.

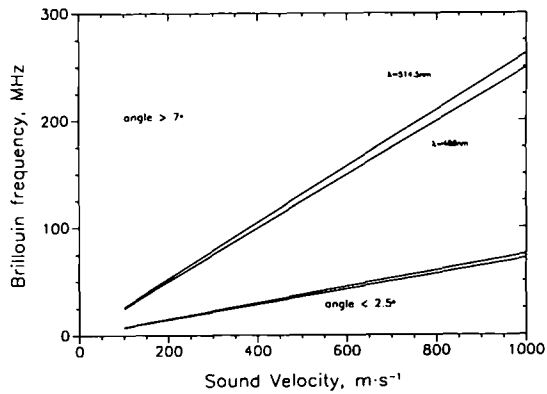

Fig. 4. Achievable sound frequencies in heterodyne Brillouin measurements.

To detect the frequency shift of the Brillouin lines by measuring in the time domain, a frequency-adapted background of sufficient intensity must be superimposed on the signal. This can be done using an optoacoustic modulator as shown in Fig. 2.

Small frequency shifts are necessary to measure sound velocities near the critical point. These can be realized by using two modulators in a line driven with different shift frequencies. If the frequency difference between one Brillouin line and the background is not too high (in general, <2 MHz), the cross-correlation function can be written

$$g(\tau) = (I_{R0} + I_R + 2I_B + I_{B0})^2 + 2I_{B0}I_B \exp(-\tau/\tau_{cB}) \cos(2\pi\, \Delta\nu\tau) \qquad (8)$$

which is a damped oscillation with a constant background:

$$g(\tau) = C + A \exp(-\tau/\tau_{cB}) \cos(2\pi\, \Delta\nu\tau) \qquad (9)$$

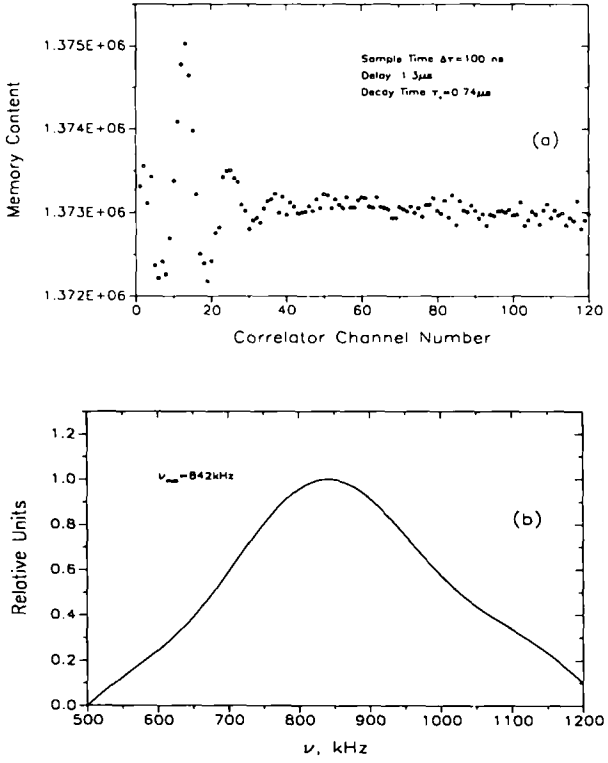

Fig. 5. (a) Heterodyne Brillouin correlogram measured with a mistuned background; (b) Fourier transform of the heterodyne Brillouin correlogram.

Here $\Delta\nu$ is the frequency difference (mistuning) between the Brillouin component and the shifted background, which can be detected accurately by a Fourier transformation of the correlogram [14]. As an example, Fig. 5 shows the result of a measurement performed in this way and the corresponding Fourier transform.

With the frequency shift of the background ν and the mistuning $\Delta\nu$, the sound velocity can be calculated to be either

$$c_s = 2\pi(\nu + \Delta\nu)/q \tag{10}$$

or

$$c_s = 2\pi(\nu - \Delta\nu)/q \tag{11}$$

The correct value can be found by performing a second measurement with another angle or another frequency.

The procedure described implies a rough knowledge of c_s, when requiring a mistuning of less than about 2 MHz at the starting point. If no value for the sound velocity is known, the best thing to do is to estimate any value and to start with a trial-and-error-procedure with a systematic variation of the frequency or the angle in such a way that, from step to step, the frequency difference is about 1 MHz. In this way, a first measurement can be found displaying a significant peak in the first correlator channels. This indicates that one is near the correct Brillouin shift. With an exact value of the sound velocity for one temperature, the next value for the next temperature may be estimated sufficiently by taking into account $(\partial c_s/\partial T) \approx -1 \ldots -10\ \mathrm{ms}^{-1} \cdot \mathrm{K}^{-1}$, depending on the sample under investigation.

3. RESULTS

3.1. Thermal Diffusivity

All measurements were performed applying the heterodyne method described above. Applying our new method of data evaluation (see Section 4.1.2), each correlogram was found to be free of systematic errors in the long time scale excluding errors due to mechanical vibrations, laser instabilities, or chemical impurities.

The measured data for the thermal diffusivity are given in Table I and displayed in Fig. 6.

Table I. Thermal Diffusivity of Boiling R125

Temperature (°C)	a (10^{-8} m^2·s^{-1})
(a) Liquid	
19.00	3.51
29.86	3.594
30.36	3.329
35.34	3.054
40.39	2.954
50.40	2.471
60.39	1.537
62.38	1.187
63.37	0.991
64.09	0.81
64.38	0.729
64.69	0.631
(b) Vapor	
33.36	10.98
38.00	8.94
43.42	7.95
48.41	6.02
53.44	4.40
58.44	2.916
63.53	1.114
64.51	0.722
65.04	0.530

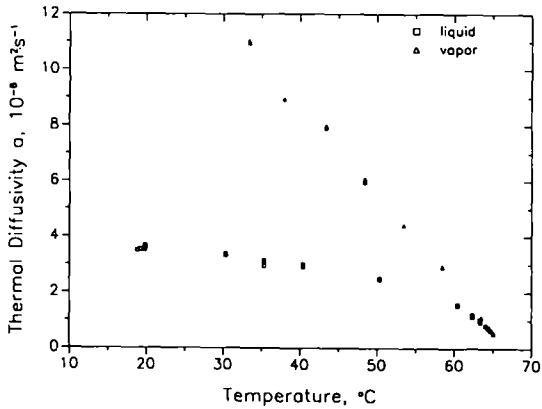

Fig. 6. Thermal diffusivity of saturated R125.

3.2. Sound Velocity

The values for the sound velocity are given in Table II and shown in Fig. 7. The corresponding frequencies may roughly be taken from Fig. 4. In no case was a significant dispersion (>0.5%) found when the applied frequency was varied.

4. DISCUSSION

4.1. Thermal Diffusivity

In measuring the thermal diffusivity four possible main error sources can be identified: (1) angle measurement, (2) determination of the decay time, (3) insufficient determination of the background contribution, and (4) temperature measurement.

Table II. Sound Velocity of Boiling R125

Temperature (°C)	c_s (m·s^{-1})
(a) Liquid	
19.96	354.02
30.38	300.80
35.34	275.45
40.39	249.32
50.39	192.32
60.38	125.67
62.38	110.54
63.38	102.02
64.10	94.57
64.38	92.62
64.70	89.62
64.99	86.88
65.19	84.75
(b) Vapor	
33.37	112.34
38.40	105.16
43.40	109.68
48.41	101.32
53.41	96.84
58.44	92.00
63.51	84.51
64.52	82.25
65.02	80.64

4.1.1. Angle Measurement

The angle is measured with an inaccuracy of less than $\pm 0.02°$. With an assumed average measurement angle of 4°, this gives a relative error of about 1%. Performing multiple measurements at different angles, this error partly averages out.

4.1.2. Determination of the Decay Time

The decay time may be calculated using a linearization method or a non-linear fit algorithm. The accuracy achieved depends mainly on two factors, the absence of systematic errors and the degree of noise. Systematic errors can occur in the first channels as short-time distortions or in the last channels as long-time errors. Short-time effects arise mostly from photomultiplier artifacts and can be suppressed completely by the calculation of the cross-correlation function with two PMTs. A short-time contribution from the Brillouin signal in general cannot be observed when measured with the heterodyne method.

To avoid long-time effects, mechanical vibrations, chemical impurities, laser instabilities, and laser-induced flow fields must be avoided very carefully. Therefore, the experimental setup is placed on a pneumatic support system providing a high stability.

Chemical impurities lead to microscopic concentration fluctuations causing an additional exponential decaying function in the measured correlogram with a decay time governed by the diffusion coefficient. This decay time is, in general, one order of magnitude longer than that of the thermal diffusivity [15].

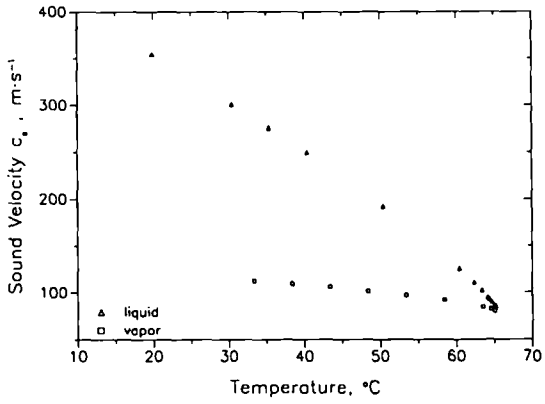

Fig. 7. Sound velocity of saturated R125.

Chemical impurities were removed from the sample to a high degree by refining the refrigerant before filling it into the pressure vessel using a rectification and adsorption process. Analysis of a R152a sample treated in this way indicated a purity of better than 99.99%. We estimate the purity of the R125 sample to reach the same level.

Besides mechanical vibrations and chemical impurities, laser-induced flow fields can also cause a long-time decay in the measured correlogram. In particular, in the critical region the laser intensity must not be too high. In all measurements the laser power was adjusted such that no change in the decay time as function of the laser intensity was observable. In the critical region, only a few milliwatts was irradiated. Higher laser intensities caused a significant long-time decay in the measurements and prevented accurate determination of the thermal diffusivity.

Because the measured fluctuations are of a stochastic nature, a finite noise on the correlogram cannot be avoided. For the best results, the decay-time average from several measurements must be used for the evaluation procedure.

Far away from the critical point the Rayleigh signal vanishes for both phases. The vapor-phase signal is in general lower than that of the liquid phase. Here the noise increases rapidly and thus the thermal diffusivity becomes more inaccurate.

The thermal diffusivity values listed in Table I represent the average of all performed measurements.

4.1.3. Insufficient Determination of the Background Contribution

Assuming a single-exponential decaying function, when starting the fit procedure, implies that the background contribution is much larger than the signal ($I_{R0}/I_R > 200$). If this is not true, two exponentially decaying functions are superimposed, yielding a factor of two in the decay times [12]. To ensure that the background contribution is sufficiently high, the contrast A/C according to Eq. (4) must be less than 0.03. Furthermore, no systematics should be recognizable in a deviation plot between measurement and calculated correlogram and the variation of the fit interval used in the evaluation procedure must not influence significantly the result of the decay time obtained. All these steps were performed carefully in the measurements presented here.

4.1.4. Temperature Measurement

The overall error of the thermal diffusivity depends also on the value of $\partial a/\partial T$. For a given temperature error the uncertainty of the thermal diffusivity diverges close to the critical point due to the very low values of the thermal diffusivity compared to the high values of $\partial a/\partial T$.

Taking into account all possible error sources explained, we estimate the inaccuracy of the thermal diffusivity measurements for a single temperature point to be within $\pm 3\%$ in the liquid phase and in the vapor phase. The inaccuracy will increase close to the critical point and for the vapor phase for temperatures below 40°C.

4.2. Sound Velocity

The frequency of the damped oscillation containing the information on the sound velocity can be detected very sensitively by Fourier transformation. Here long-time signals usually cause only minor errors and can be suppressed to a high degree using a strong coherent background signal [14].

The residual error of the evaluation procedure and of the angle measurement can be estimated from the scatter of the results of several measurements at one temperature. Here an error of approximately $\pm 0.5\%$ has been found for most temperatures. Only near the critical point, where the Brillouin signal vanishes, does the accuracy decrease. The overall error for the sound velocity can be estimated by adding the inacuracy of the temperature measurement.

ACKNOWLEDGMENTS

The authors gratefully acknowledge financial support by the Deutsche Forschungsgemeinschaft. We also thank Du Pont de Nemours for providing us with the refrigerant R125 and for analyzing the refined fluid.

REFERENCES

1. R. Krauss, *MIDAS Database for Thermophysical Properties*, Lehrstuhl für Technische Thermodynamik und Thermische Verfahrenstechnik (Universität Stuttgart, Stuttgart, April 1993).
2. A. Leipertz, *Int. J. Thermophys.* **9**:897 (1988).
3. M. Hendrix, A. Leipertz, M. Fiebig, and G. Simonsohn, *Int. J. Heat Mass Transfer* **30**:333 (1987).
4. G. Wu, M. Fiebig, and A. Leipertz, *Int. J. Heat Mass Transfer* **31**:1471 (1988).
5. G. Wu, M. Fiebig, and A. Leipertz, *Int. J. Heat Mass Transfer* **31**:2555 (1988).
6. B. Hinz, G. Simonsohn, M. Hendrix, G. Wu, and A. Leipertz, *J. Modern Opt.* **34**:1093 (1987).
7. G. Simonsohn and F. Wagner, *Opt. Lett.* **14**:110 (1989).
8. G. Simonsohn and F. Wagner, *J. Phys. D Appl. Phys.* **22**:1179 (1989).
9. A. Leipertz, K. Kraft, and G. Simonsohn, *Fluid Phase Equil.* **79**:201 (1992).
10. G. Simonsohn, *Opt. Acta* **30**:1675 (1983).

11. B. J. Berne and R. Pecora, *Dynamic Light Scattering* (Wiley, New York, 1976).
12. M. Hendrix, *Photonen-Korrelationsspektroskopie als optisches Standardverfahren zur Messung der Temperaturleitfähigkeit reiner Flüssigkeiten in einem weiten Temperatur- und Druckbereich* (Dr-Dissertation, Ruhr-Universität Bochum, 1984).
13. S. Will and A. Leipertz, *Appl. Opt.* **32**:3813 (1993).
14. K. Kraft and A. Leipertz, *Appl. Opt.* **32**:3886 (1993).
15. W. Krahn, G. Schweiger, and K. Lucas, *J. Phys. Chem.* **87**:4515 (1983).